Wang *et al.*
Chinese Journal of Mechanical Engineering (2022) 35:39
https://doi.org/10.1186/s10033-022-00711-6

Chinese Journal of Mechanical Engineering

ORIGINAL ARTICLE

Open Access

Modelling and Dynamic Characteristics for a Non-metal Pressurized Reservoir with Variable Volume

Pei Wang[1], Jing Yao[1,2,3*], Baidong Feng[1], Mandi Li[1] and Dingyu Wang[1]

Abstract

With the increasing demand to reduce emissions and save energy, hydraulic reservoirs require new architecture to optimize their weight, space, and volume. Conventional open reservoirs are large, heavy, and easily polluted, and threaten the operation of hydraulic systems. A closed reservoir provides the advantages of small volume and light weight, compared to open reservoirs. In this study, a non-metallic pressure reservoir with variable volume is designed and manufactured for closed-circuit hydraulic systems. The reservoir housing is made of rubber, and the Mooney-Rivlin model is chosen based on the rubber strain properties. The FEA simulation for the reservoir is performed using ANSYS Workbench to obtain the structural stiffness. The major contribution is the establishment of mathematical models for this reservoir, including the volume equation changing with height, flow equation, and force balance equation, to explore the output characteristics of this reservoir. Based on these results, simulation models were built to analyze the output characteristics of the reservoir. Moreover, the test rig of a conventional hydraulic system was transformed into a closed-circuit asymmetric hydraulic system for the reservoir, and preliminary verification experiments were conducted on it. The results demonstrate that the designed reservoir can absorb and discharge oil and supercharge pump inlet to benefit system operation. The changes in the volume and pressure with displacements under different volume ratios and frequencies were obtained, which verified the accuracy of the mathematical models. Owing to its lightweight design and small volume, the reservoir can replace conventional open reservoirs, and this lays a foundation for future theoretical research on this reservoir.

Keywords: Hydraulic reservoir, Variable volume, Pressure reservoir, Non-metal, Lightweight

1 Introduction

Hydraulic transmission is crucial in aerospace, heavy machinery, engineering machinery, and other industries [1–5]. Hydraulic systems often rely on large and heavy reservoirs in mobile hydraulic machinery. It is one of the components with the highest potential for weight reduction [6]. The lighter weight of hydraulic reservoirs can improve the power-to-weight ratio of mobile hydraulic machinery and reduce power consumption, achieving energy conservation and emission reduction. The purpose of this study is to effectively reduce the mass and volume of hydraulic reservoirs while meeting the strict requirements of hydraulic systems.

Open and closed reservoirs are utilized in the hydraulic systems. Although open reservoirs are widely utilized, they are not applied in high-altitude environments and are restricted to mobile hydraulic machinery. To address this challenge, closed reservoirs have installed a pressure-driven device that can relatively stabilize the oil pressure at the pump inlet and enable the hydraulic system to work at a high altitude or in harsh environment [7–10]. Compared with open reservoirs, closed reservoirs have a smaller volume and mass, and are more widely utilized

*Correspondence: jyao@ysu.edu.cn
[1] School of Mechanical Engineering, Yanshan University, Qinhuangdao 066004, China
Full list of author information is available at the end of the article

in mobile hydraulic machinery. There is an urgency to design a new type of closed reservoir with small volume and light weight, to meet the lightweight and pressure requirements of the hydraulic system.

There are several types of closed reservoirs, and the difference between them is mainly reflected in pressure-driven methods. The pressure-driven devices of a closed reservoir are mainly divided into hydraulic, spring, and pneumatic drives. Parker's closed metal reservoir is designed to connect the system pressure to the reservoir drive interface. In addition, system pressure can be converted into a stable low-pressure output; however, it occupies a large space and has a large mass. Spring-driven [11, 12] closed reservoirs rely on a spring force to exert pressure on the oil, but their structure is relatively complex and difficult to process and manufacture. Another type of closed reservoir utilizing a pneumatic drive [13–19] is protected by a metal housing, but the container inside is coated in rubber skin. Gas is filled between the metal housing and rubber skin to establish the driving pressure, but it is sensitive to temperature, which affects the normal operation of the hydraulic system, such as the contact booster hydraulic [20] and air-bag isolated booster hydraulic tanks [21]. There are also closed reservoirs with special structural forms, such as a vacuum reservoir with variable capacity, following the movement of actuators [22]. The corrugated elastic lining and housing form a closed capacity cavity, and the bellows produce telescopic action in the opposite direction, altering the volume [23]. Its disadvantage is that the pressure of the output oil is nonlinear and unsuitable for hydraulic systems that require stable pressure. As described above, the complex structure, large volume, large mass, and nonlinear output pressure of the existing closed reservoir are still not conducive for reducing the weight and space of the hydraulic system.

Generally, conventional hydraulic reservoirs are made of metal materials with simple structures, but larger volumes and weights. Non-metal reservoirs have garnered significant attention owing to their lightweight development. A few companies have researched and developed reservoirs using special materials for various functions. ARGO-HYTOS [24] developed an injection-plastic reservoir with a filtering function. Fuel Safe [25] developed a material for designing a collapsible aerial fuel transport container. It is constructed with multiple layers of ballistic nylon cords and a rugged rubberized polymer coating, but not suitable for hydraulic systems. Turtle-Pac [26] manufactured aircraft tanks using unique fabrics and technologies. It is lightweight, convenient to fold, compact, and is tested at 5 PSI during quality control tests. In addition, Smart Reservoir [27], a company in Canada, produced another type of reservoir with the features of lighter mass, smaller volume, and linear output. It has already been applied in various fields, but the effect of rubber on reservoir performance is unclear. Currently, most of the research on lightweight non-metal hydraulic reservoirs are abroad, but seldom research has been conducted on its characteristics and material.

Therefore, considering the particularity of rubber material, this research takes the variable volume and pressure reservoir (VVPR) as the research object, focuses on the establishment of mathematical models for dynamic characteristics, and explores the interaction between the system parameter and VVPR by simulation and experiments. This paper is divided into four parts: ① Composition and principle of the VVPR. ② Strain properties and structural stiffness of reservoir rubber. ③ Modeling and simulation of the VVPR using AMESIM and MATLAB joint simulation methods. ④ Performance analysis of the VVPR in closed-circuit hydraulic system on test platform. It is important to investigate this closed reservoir to replace open reservoirs in numerous applications, which provides a theoretical basis for further research.

2 Reservoir Description

2.1 Working Principle

The VVPR is sealed, airless, and slightly pressurized, with small volume, light weight, low pollution, and portability. It comprises upper and lower covers, rings, connecting rods, rubber housing, springs, pillars, and other components, as illustrated in Figure 1.

The connecting rod is fixed to the upper cover, and the rod and spring in the pillar move with reservoir motion. The spring is always in a compressed state with a downward force on the connecting rod. Through the interaction of the spring and internal pressure of the oil, the reservoir can achieve the functions of absorbing and discharging oil.

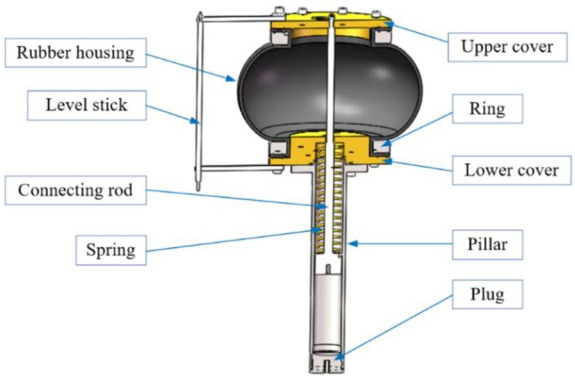

Figure 1 Composition of the reservoir (VVPR)

The VVPR designed in this study plays the role of differential volume compensation in closed-circuit asymmetric hydraulic systems by its own variable volume. In the working cycle of the reservoir, expansion and contraction occur as actuator movement changes. The process of oil absorption and discharge with the expansion and compression of the rubber housing can be achieved using the spring force. As illustrated in Figures 2 and 3, the working principle of the VVPR in a closed-circuit valve-controlled asymmetric hydraulic system is described as follows.

A closed-circuit valve-controlled asymmetric hydraulic system comprises a hydraulic pump, single-rod cylinder, direction valve, and VVPR. The oil absorption conditions of the reservoir are illustrated in Figure 2. In the retraction process of the cylinder, the oil from the outlet of the hydraulic pump enters the rod chamber of the hydraulic cylinder, and the oil in the rodless chamber enters the suction port of the hydraulic pump through the directional valve. However, owing to the different volumes of oil in the two chambers of the hydraulic cylinder, part of the oil in the rodless chamber enters the reservoir.

The oil discharge conditions of the VVPR are illustrated in Figure 3. During the extension of the cylinder, the oil from the outlet of the hydraulic pump enters the rodless chamber of the hydraulic cylinder, and the oil in the rod chamber enters the suction port of the hydraulic pump through the directional valve. The oil in the VVPR is replenished into the inlet of the pump.

A VVPR was preliminarily designed and manufactured to investigate the reservoir characteristics. The main parameters of the VVPR are as follows: ① Its working pressure is under 0.06 MPa, working volume is 5 L, and structure volume is 9.63 L. ② It is 580 mm in height and 400 mm in width. ③ Its mass is only 13.2 kg, owing to the smaller working cavity made of rubber material.

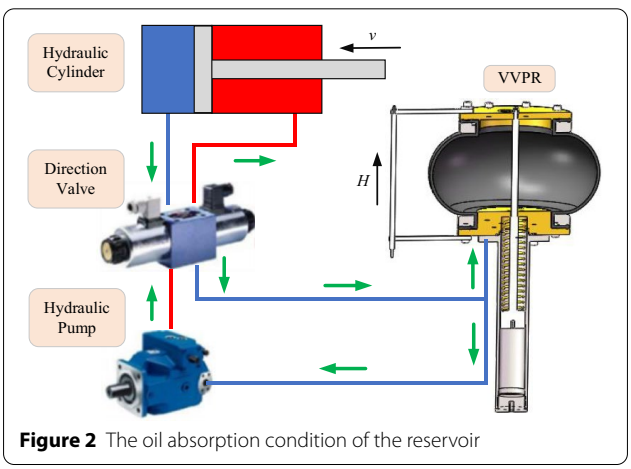

Figure 2 The oil absorption condition of the reservoir

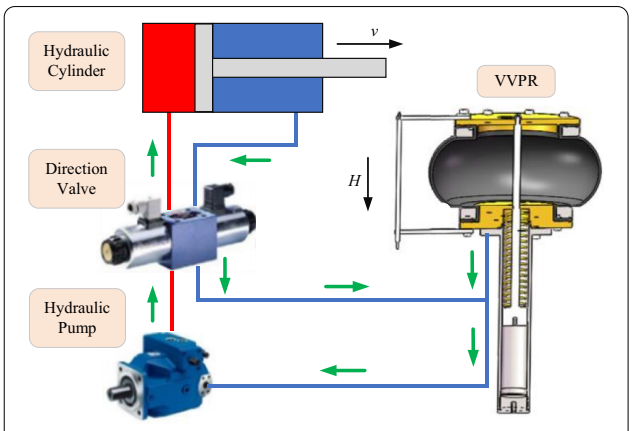

Figure 3 The oil discharging condition of the reservoir

2.2 Rubber Strain Properties and its Constitutive Equation

The rubber housing material utilized in the VVPR is a hyperplastic material that may affect the VVPR dynamic characteristics. Therefore, the physical properties of these materials should be described based on their elasticity and deformation.

To determine the correct mathematical model (constitutive equation) to describe rubber physical properties in the reservoir and define the system dynamic properties, uniaxial tension tests with six rubber samples were conducted at 20 °C (environment temperature), as illustrated in Figure 4. There are several mathematical models to describe the physical properties of hyperplastic materials, including the Mooney-Rivlin model, Ogden, and Yeoh models, but not all of them are suitable for specific hyperplastic materials [28]. The rubber stress and strain data from the uniaxial tension test results on the test pieces were utilized for comparison with the FEA simulation results from ANSYS Workbench for different rubber models, and the results are illustrated in Figure 5.

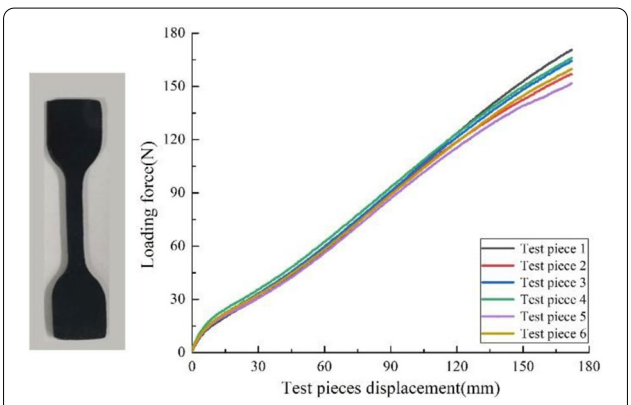

Figure 4 Uniaxial tension test results at 20 ℃

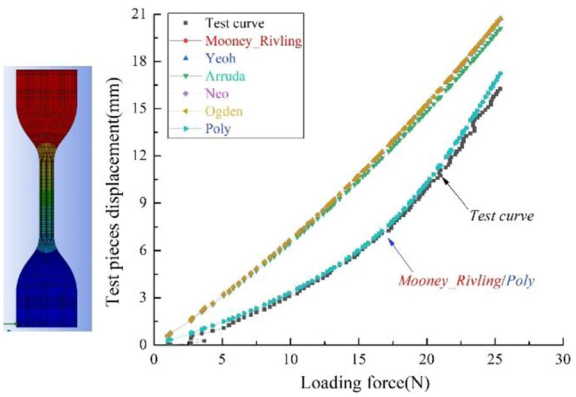

Figure 5 The test pieces displacement curve of FEA simulation results and test result

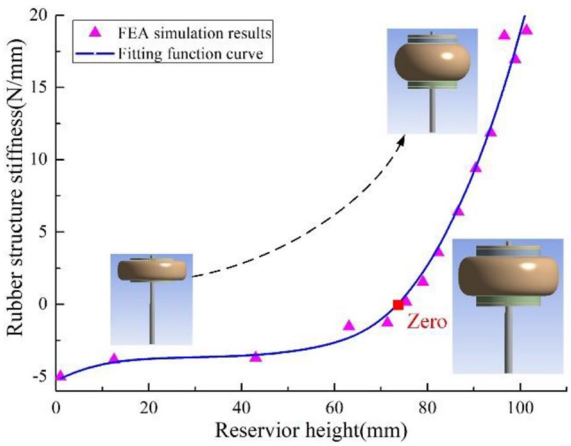

Figure 6 Rubber structural stiffness

Table 1 Parameters of rubber Mooney-Rivlin model

Rubber parameter	Value(MPa)
Material constant C10	− 2.4201
Material constant C01	4.2156
Material constant C20	− 0.0035296
Material constant C11	0.027367
Material constant C02	0.81943
Incompressibility parameter	0

Table 2 The stiffness fitting function and parameters

Parameters	Value
K_1(N/mm)	$f(x)=a_1x^4+a_2x^3+a_3x^2+a_4x+a_5$
a_1(N/mm^5)	2.401×10^{-7}
a_2(N/mm^4)	4.105×10^{-5}
a_3(N/mm^3)	− 0.006157
a_4(N/mm^2)	0.2066
a_5(N/mm)	− 5.315

It can be observed that there are constitutive models that fit the test data well, i.e., Mooney-Rivlin, and Poly, which can describe the basic rubber hyperplastic properties. In this study, the Mooney-Rivlin model was selected for the next simulation step, and its parameters are presented in Table 1.

2.3 Rubber Structural Stiffness of VVPR

Since the hyperplastic material is elastic, the stiffness of the structure on the upper cover should be provided. Once the constitutive model of rubber and the structure of the reservoir are determined, the rubber structural stiffness of the VVPR can also be obtained. Therefore, FEA simulation on ANSYS Workbench was performed by constantly changing the force F on the connecting rob and simulating the displacement of the upper cover x. The rubber structural stiffness K_1 of VVPR can be calculated with Eq. (1).

$$K_1 = \frac{\Delta F}{\Delta x}, \tag{1}$$

The rubber structural stiffness of the VVPR when a force acts on the upper cover is illustrated in Figure 6. It can be observed that as the reservoir height increases, the stiffness also increases.

According to simulation results, the fitting function of K_1 has also been obtained using a quartic polynomial curve function with a corresponding fitting precision of R-square = 0.982 and RMSE = 0.1389. The stiffness fitting functions and parameters are presented in Table 2.

3 Modelling and Simulation

The VVPR continuously absorbs and discharges oil in its working cycle with the movement of the hydraulic cylinder, thereby affecting the changes in its volume and pressure. Volume and pressure are important parameters in the performance of the VVPR; thus, mathematical models must be built for further simulation analysis of the changes in volume and pressure during the working cycle.

3.1 Force Balance Equation

The VVPR can be equivalently treated as a single-degree-freedom system with spring-mass-damping, which can be simplified to the model illustrated in Figure 7.

In Figure 7, H is the height of the VVPR; K, K_1, and K_2 are the stiffness of the spring, rubber structure, and oil, respectively; m is the mass of the moving parts of the VVPR, A is the area of the upper cover, p is the pressure

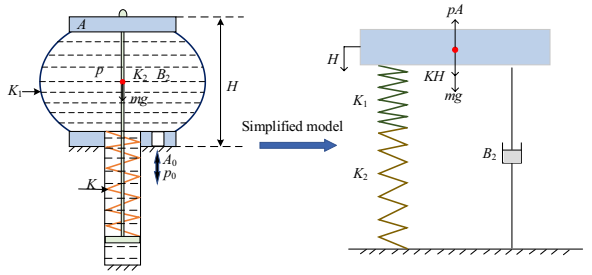

Figure 7 The dynamic model of the VVPR

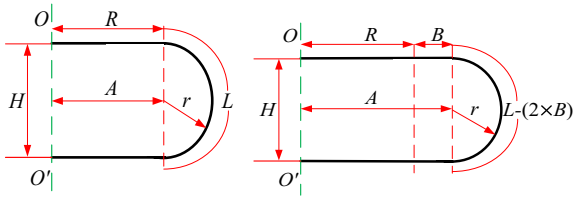

(a) Uncompressed volume (b) Compressed volume

Figure 8 The dimension diagram of the rubber housing

inside the VVPR, and B_2 is the movement damping of the VVPR.

The oil stillness can be obtained by Eq. (2):

$$\begin{cases} \Delta V = \dfrac{V}{\beta_e}\Delta p, \\ \Delta V = A\Delta H, \ \Rightarrow K_2 = \dfrac{\beta_e A^2}{V}. \\ K_2 = \dfrac{\Delta pA}{\Delta H}, \end{cases} \tag{2}$$

The damping coefficient B_2 can be expressed as Eq. (3):

$$B_2 = 8\pi\mu H, \tag{3}$$

where the $\mu = \mu_0 \cdot e^{\alpha \cdot p}$, $\mu_0 = 0.35$ Pa · s, and $\alpha = (0.015 \sim 0.35)\text{MPa}^{-1}$[29, 30].

When the VVPR operates by oil absorption and discharge, the upper cover exerts a force on the oil-generating pressure p. According to the dynamic model, this study considers the upper cover as the research object, and the force balance equation is established by considering the inertial force, viscous damping force, spring force, and internal pressure on the upper cover. Hence, the force balance equation can be expressed as Eq. (4):

$$Ap = m\frac{\mathrm{d}^2H}{\mathrm{d}t^2} + B_2\frac{\mathrm{d}H}{\mathrm{d}t} + \left(K - \frac{K_1 \cdot K_2}{K_1 + K_2}\right)H + mg. \tag{4}$$

The first term on the right side of Eq. (4) is the inertial force, second term is the viscous damping force, and final term is the elastic force exerted by the spring, rubber, and oil.

3.2 Volume Equation

As the VVPR moves, the volume changes with the height. Volume calculation is crucial for obtaining the change in height; its dimensions in the vertical plane are illustrated in Figure 8.

In Figure 8, r is the radius, L is the arc length, R is the radius of the upper cover, A is the distance from the central axis to the arc center, and B is the line segment after arc deformation. The relationships between these variables can be expressed as Eq. (5).

$$\begin{cases} r = \dfrac{H}{2}, \\ B = \dfrac{L - \pi r}{2}, \\ A = B + R. \end{cases} \tag{5}$$

Hence, the volume equation can be expressed as Eq. (6).

$$V(H) = \pi H\left\{\frac{1}{6}H^2 + R^2 + \frac{1}{4}R\pi H + \left(\frac{L}{2} - \frac{\pi H}{4}\right)\left(\frac{L}{2} + 2R\right)\right\}. \tag{6}$$

Furthermore, the relationship between the volume V and height H was drawn based on the Newton iteration method in MATLAB, as illustrated in Figure 9.

3.3 Flow Continuity Equation

Some assumptions are made to establish the flow continuity equation of the VVPR: ① pressure loss and pipeline dynamic characteristics of components other than the VVPR are not considered; ② the elastic modulus of

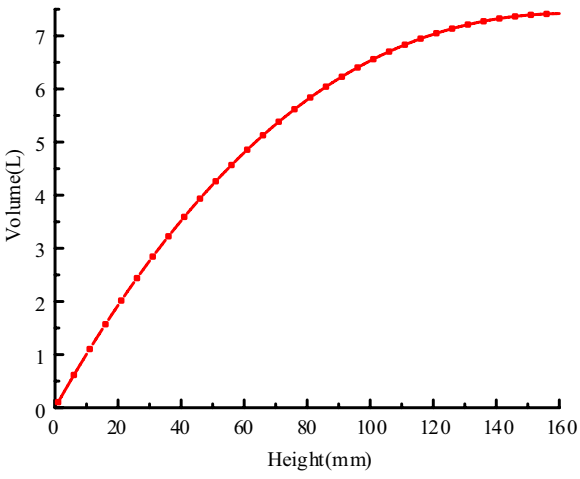

Figure 9 The simulation curve of volume change with height

oil and oil temperature are constant; and ③ the reservoir leakage is a laminar flow. Hence, the flow continuity equation is expressed as Eq. (7):

$$q = \frac{\mathrm{d}V}{\mathrm{d}t} + C_{ep}p + \frac{V}{\beta_e}\frac{\mathrm{d}p}{\mathrm{d}t}. \tag{7}$$

The first term on the right side of Eq. (7) represents the volume change of the VVPR during operation, second term represents the flow rate change caused by leakage, and third term represents the flow rate change due to compression.

3.4 Simulation Analysis

To explore the performance of the VVPR in the system and effect of the VVPR on the system, joint models of the VVPR in MATLAB and a closed-circuit hydraulic system in AMESIM were built for their interaction with different working parameters. The main simulation parameters are presented in Table 3.

The initial volume was set as 3.7 L, and the ratio between the actual working volume ΔV and maximum working volume V is defined as the volume ratio, expressed as Eq. (8):

$$\alpha = \frac{\Delta V}{V}. \tag{8}$$

The relationship between the actual working volume ΔV of the VVPR and hydraulic cylinder displacement y is expressed as Eq. (9):

$$\frac{\pi d^2}{4} y = \Delta V. \tag{9}$$

In this study, the hydraulic cylinder is given a sine displacement reference to form the volume difference between extension and retraction. The corresponding values of the volume ratio, stroke, and amplitude are presented in Table 4.

Table 3 Simulation parameters

Name	Parameter	Value
Cylinder	Diameter of rod d(mm)	90
	Diameter of piston D(mm)	110
	Stroke of cylinder S(mm)	800
Reservoir	Stiffness of spring K(N/mm)	13.63
	Mass m(kg)	6
	Damping B_2(N· s/mm)	0.01
	Elastic modulus β_e(MPa)	700

Table 4 The relationship among the volume ratio, stroke, and amplitude

Volume ratio	Stroke(mm)	Amplitude(mm)
0.05	39.30	19.65
0.1	78.60	39.30
0.2	157.20	78.60
0.3	235.80	117.90
0.4	314.40	157.20
0.5	393.00	196.50
0.6	471.60	235.80
0.7	550.20	275.10

The displacement of the hydraulic cylinder was set as a sine curve with amplitudes of 117.90 mm at 0.016 Hz, to analyze the output characteristics of the VVPR. As can be observed from Figures 10 and 11, the height and volume of the VVPR gradually increases when oil is absorbed. At half a cycle, the flow rate into the VVPR is 0, and both the volume and height of the VVPR reach their maximum values, but the pressure of the VVPR does not. During the oil discharge, the volume and height of the VVPR gradually decreases, while the pressure of the VVPR increases.

Through the simulation analysis, it is determined that the volume and height of the VVPR change with the flow rate described earlier, but the change in the pressure of the VVPR has a certain delay. This may be caused by the rubber material characteristics and damping force.

3.4.1 Performance Analysis at Different Volume Ratios

In this section, the VVPR performance with different volume ratios is analyzed by altering the amplitudes of the sinusoidal displacements. The cylinder

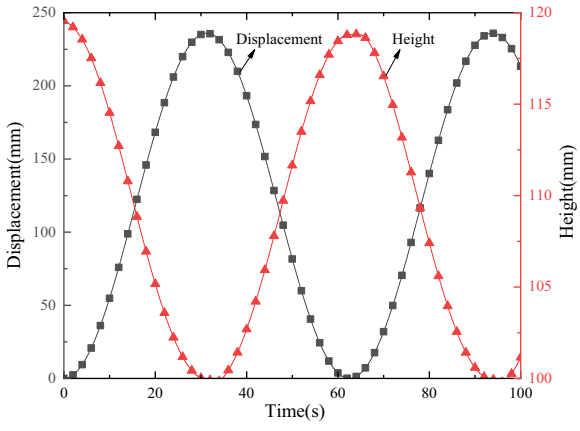

Figure 10 The height changes with displacement

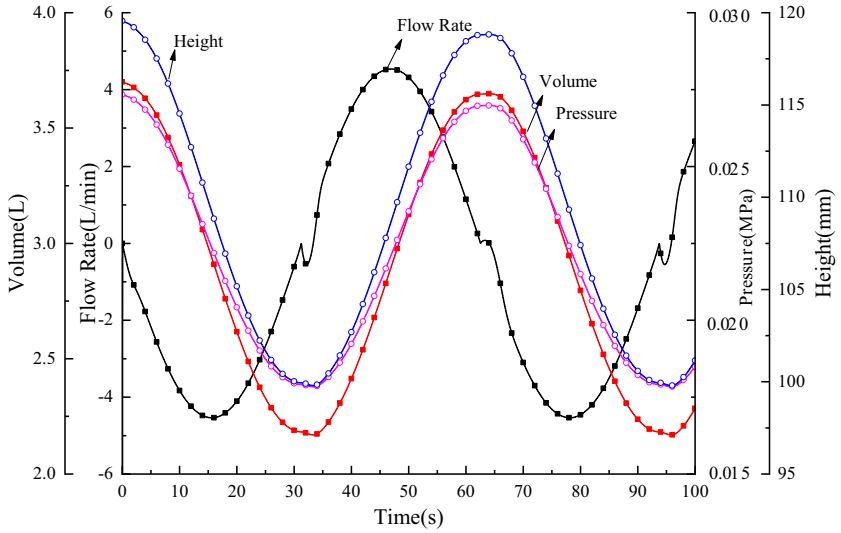

Figure 11 The changes in the main parameters of the VVPR

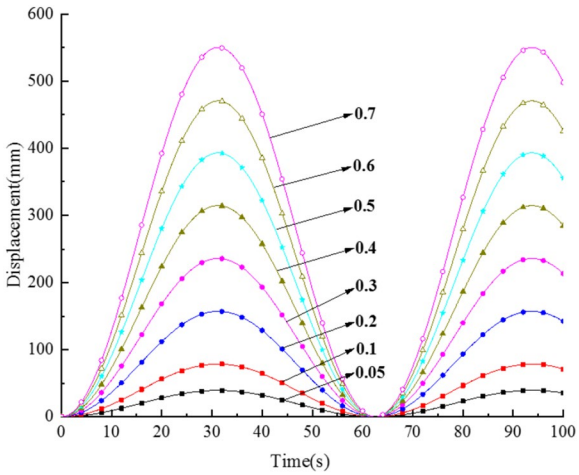

Figure 12 Displacement curve of hydraulic cylinder

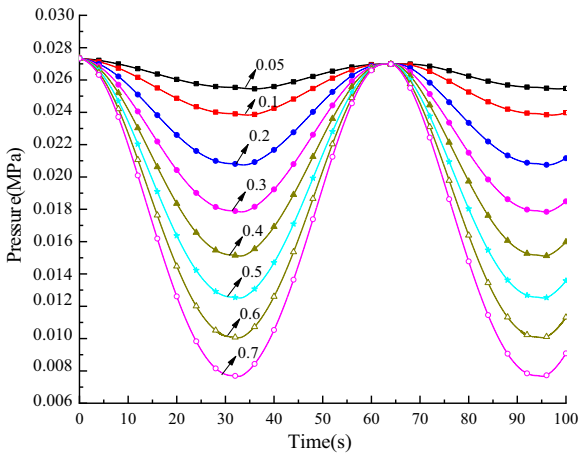

Figure 13 Changes in pressure at different ratios

displacement is selected as a sine curve at 0.016 Hz, and the volume ratios of the reservoir are set as 0.05, 0.1, 0.2, 0.3 0.4, 0.5, 0.6 and 0.7, changed by the different strokes.

Figures 12, 13, 14 and 15 illustrate that the frequencies and amplitudes of the pressure and volume change with displacement, thereby displaying a positive relationship. This illustrates that the reservoir achieved the function of flow inlet and outlet with the extension and retraction of the cylinder. The cylinder displacement tracked the reference well, proving that the introduction of the VVPR had no effect on the output characteristics of the system.

3.4.2 Performance Analysis at Different Frequencies

In this section, we further explored the effect of frequency on the output characteristics of the reservoir. The

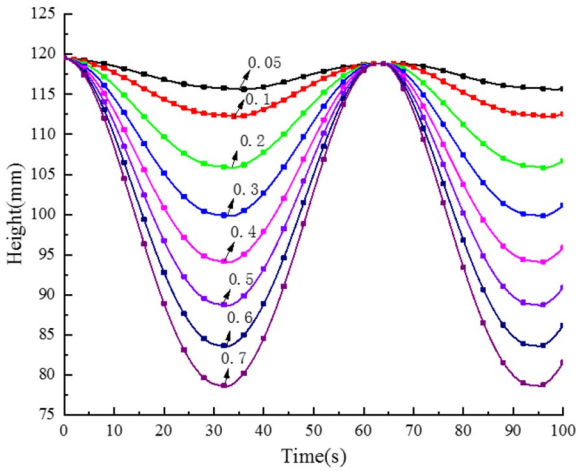

Figure 14 Changes in height at different ratios

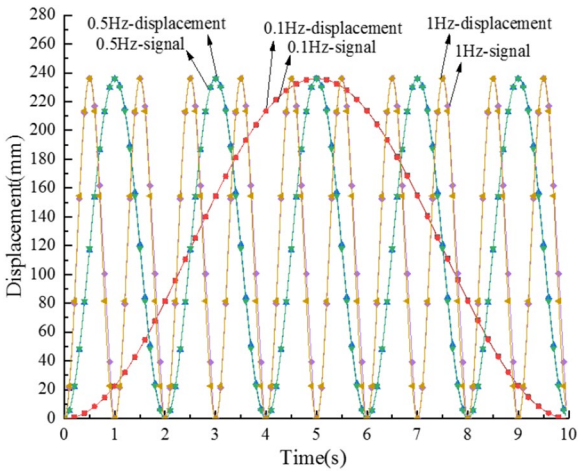

Figure 16 Displacement curves of hydraulic cylinder

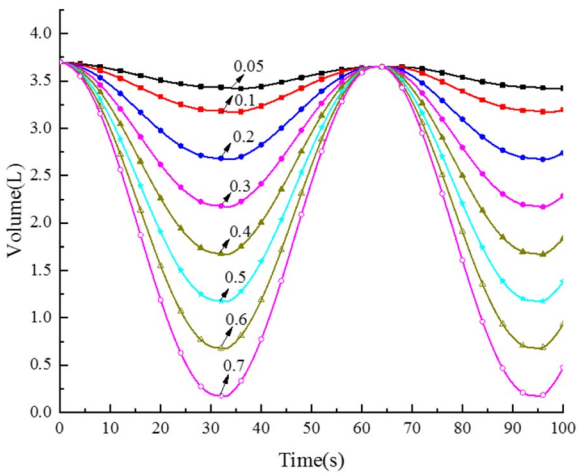

Figure 15 Changes in volume at different ratios

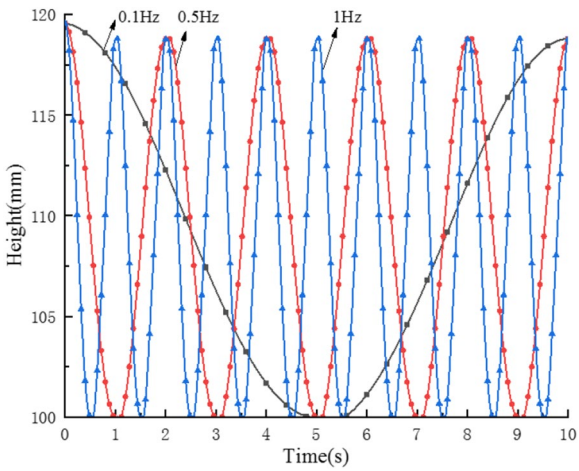

Figure 17 Changes in height at different frequencies

volume ratio was set to 0.3, and the working frequencies were selected as 0.1 Hz, 0.5 Hz, and 1 Hz to simulate the closed-circuit hydraulic system.

It can be observed from Figures 16, 17, 18 and 19 that the frequencies of the pressure, volume, and height are the same as the displacement. When the cylinder was extended, the reservoir provided the system with oil. The pressure, volume, and height decrease with increasing displacement. In contrast, the system provided oil to the reservoir when the cylinder was retracted. The pressure, volume, and height increased with decreasing displacement. This indicated that the reservoir achieved the function of flow inlet and outlet with the extension and retraction of the cylinder. The cylinder displacement tracked the reference well, proving that the introduction of the VVPR had approximately no effect on the system characteristics.

4 Experimental Results and Discussion

The test rig was transformed based on a conventional open hydraulic system to verify the accuracy of the mathematical models and simulation analysis, as illustrated in Figure 20. The test platform can achieve an open-or

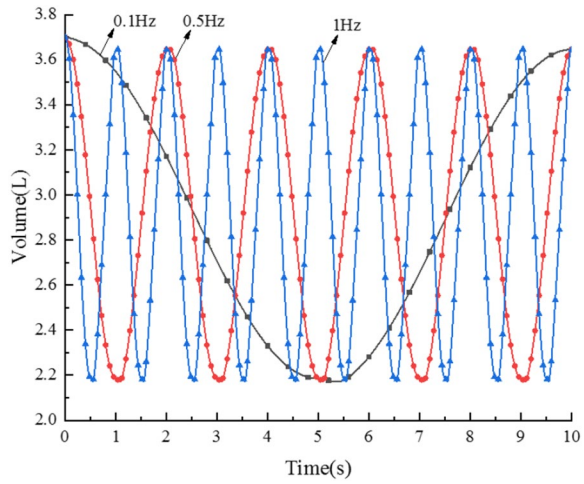

Figure 18 Changes in volume at different frequencies

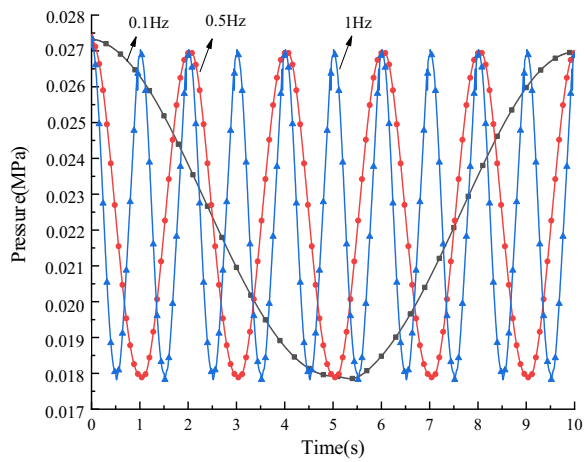

Figure 19 Changes in pressure at different frequencies

closed-circuit hydraulic system by the on/off of the shut-off valve (2.2) and union tee (3). Before the VVPR worked normally, it needed to replenish oil by opening 2.2 and 2.3 in retraction to discharge the internal air and set an initial volume (3.7 L in this study) by the open-circuit hydraulic system. The VVPR can then work normally to compensate for the volume difference of the cylinder in the closed-circuit hydraulic system.

The parameters of the test rig and main parameters between the conventional open reservoir and designed closed reservoir are presented in Table 5. In this study, volume and mass were dramatically reduced by approximately 98% and 94%, respectively.

4.1 Repeatability Analysis

In this section, static tests are conducted to explore the pressure and volume repeatability.

It can be observed from Figures 21 and 22 that the rubber housing exhibits a hysteresis phenomenon in the rising and falling processes, and the pressure curve is particularly obvious. However, the test volume-height curve is basically coincident, and the error of the pressure repeatability is within 0.002 MPa. Both the pressure and volume characteristics have high coincidence and repeatability in the three tests, which proves the volume and pressure performance and stability of the rubber material.

4.2 Experiment Analysis

To explore the relationship between the changes in pressure, height, and volume of the VVPR and the flow rate of the VVPR, the volume ratio was set to 0.3 with an initial value of 3.7 L. A sine reference with a 118 mm amplitude of 0.016 Hz was selected to test the performance of the VVPR. The relationships between the height, pressure, and volume of the VVPR were obtained. The key parameter changes in the working cycle are illustrated in Figures 22 and 23, respectively.

It can be observed from Figures 23 and 24 that the height of the VVPR can follow the displacement of the cylinder. When the cylinder was extended and retracted, the height decreased and increased at the same frequency, with approximately no hysteresis. Meanwhile, the changes in pressure and volume had the same frequency and tendency as the height. The experimental results indicated a similar tendency for these parameters as the simulation results, and it was demonstrated that the mathematical models and simulation results were corrected. Furthermore, the performance was analyzed at different working volumes and frequencies.

4.2.1 Performance Analysis at Different Volume Ratios

To verify the processes of parameter changes in the VVPR under different working volume ratios, the strokes of the cylinder were set to different values in the process of extension and retraction, to achieve different working volume ratios (0.05, 0.1, 0.2, 0.3, 0.4, 0.5 and 0.6) at 0.016 Hz. The corresponding strokes were calculated using Eq. (9). The test results are as follows.

It can be observed from Figures 25, 26, 27 and 28 that the change tendency in pressure, height, and volume of the VVPR under different working volume ratios are the same; i.e., the performance of the VVPR under different

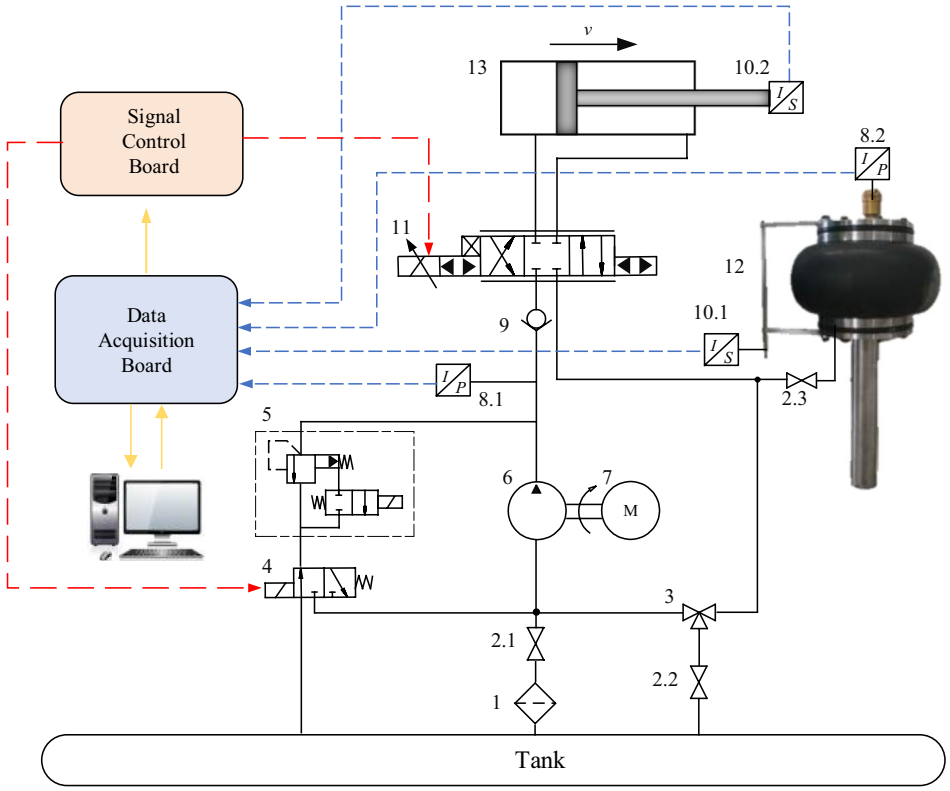

Figure 20 Principle of VVPR dynamic test. 1. Filter; 2. Shut-off valves; 3. Union tee; 4. Direction valve; 5. Unloading relief valve; 6. Hydraulic pump; 7. Electrical motor; 8. Pressure sensors; 9. One-way valve; 10. Displacement sensors; 11. Proportional reverse valve; 12. VVPR; 13 Hydraulic cylinder

Table 5 Main parameters of the test platform

Name	Parameter	Value
System	Flow rate(L/min)	20
Cylinder	Diameter of rod(mm)	90
	Diameter of piston(mm)	110
	Stroke of cylinder(mm)	475
	Difference in volume(L)	3
Open Reservoir	Length(mm)	1100
	Width(mm)	700
	Height(mm)	760
	Volume(L)	590
	Mass with oil(kg)	383.6
Closed Reservoir	Stiffness of spring(N/mm)	13.63
	Total height (mm)	580
	Width(mm)	400
	Structural volume (L)	9.63
	Mass with oil(kg)	21.28

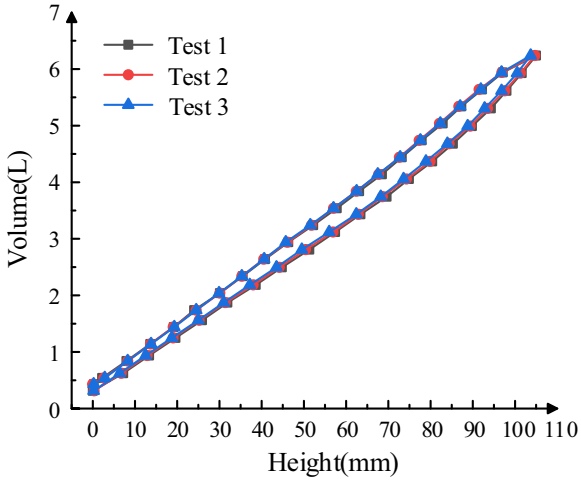

Figure 21 Volume repeatability

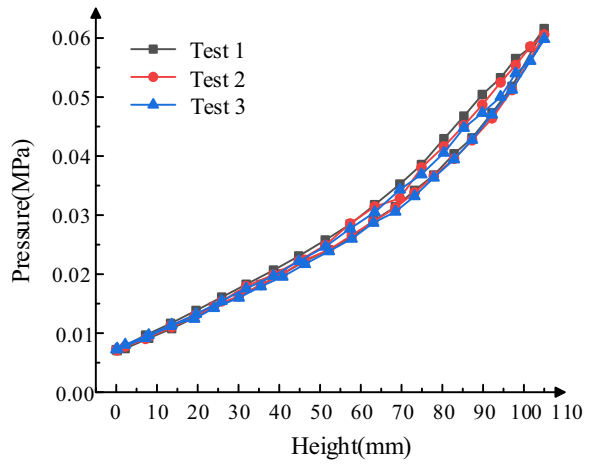

Figure 22 Pressure repeatability

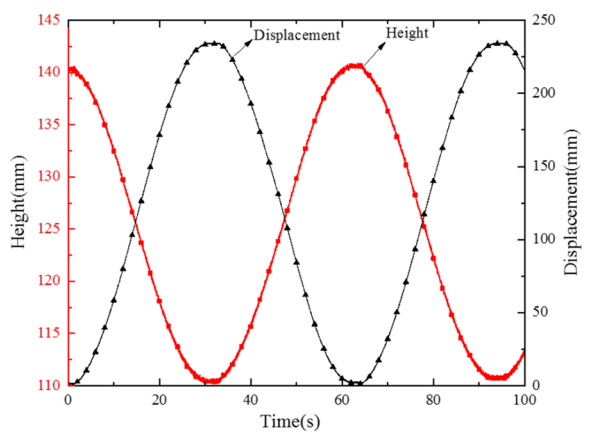

Figure 23 Change in height of the VVPR as displacement of the cylinder

working volume ratios does not change, only the variation range of these parameters changes. This is consistent with the earlier simulation findings, suggesting that the performance of the VVPR is stable at different volume rat ios.

4.2.2 Performance Analysis at Different Volume Ratios

To analyze the performance of the VVPR at different frequencies, sinusoidal signals with a working volume ratio of 0.1, and frequencies of 0.05 Hz and 0.067 Hz were selected for testing.

It can be observed from Figures 29, 30, 31 and 32 that the height, volume, and pressure of the VVPR change with the displacement of the hydraulic cylinder. The working frequencies of the VVPR also changed with those of the hydraulic cylinder. At different working frequencies, the changes in the height, volume, and pressure of the VVPR were the same as those in the displacement of the cylinder. This is consistent with earlier simulation findings, suggesting that the performance of the VVPR is stable at different frequencies.

5 Conclusions

(1) A new type of non-metallic pressure hydraulic reservoir with variable volume was manufactured and analyzed in a closed-circuit asymmetric hydraulic system, and its main components and working principles were introduced.

(2) The rubber structural stiffness was obtained via FEA simulation, based on the Mooney-Rivlin model. Furthermore, mathematical models of the reservoir were established, including volume, flow, and force balance equations. Besides, MATLAB and AMESIM joint simulation models were built for the VVPR.

(3) Tests were conducted, and the results demonstrated that the pressure, height, and volume change with the displacement frequencies of the cylinder under different volume ratios and frequencies, which verified the accuracy of the mathematical models.

(4) The test volume-height curves were basically coincident, error of pressure repeatability was within 0.002 MPa, and its volume and pressure performance were stable by repeatability tests. The changes in pressure had no effect on the displacement output characteristics and provided pressure for the pump inlet, which is beneficial for improving the service life of the pumps and the performance of the system.

(5) The designed VVPR would cut the volume and weight dramatically by approximately 98% and 94%, respectively, and could replace conventional open reservoirs in numerous applications. However, it also faced the challenge of heat generated by the closed hydraulic system.

Because this is the beginning of a research project on the VVPR, there is naturally much basic work that needs to be done. In addition, there are some limitations that need to be addressed to match the parameters

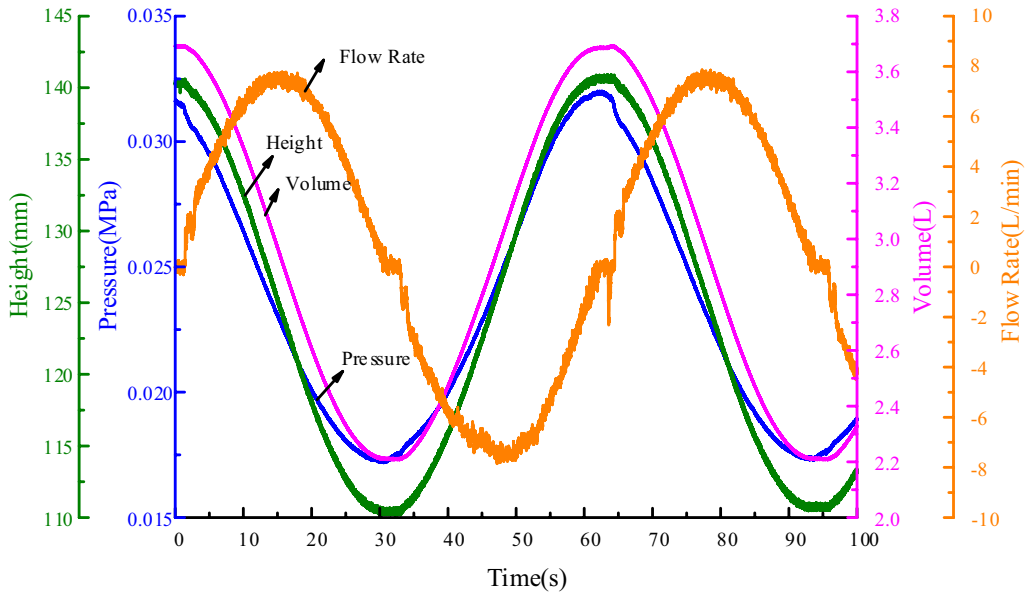

Figure 24 The changes in the main parameters of the VVPR

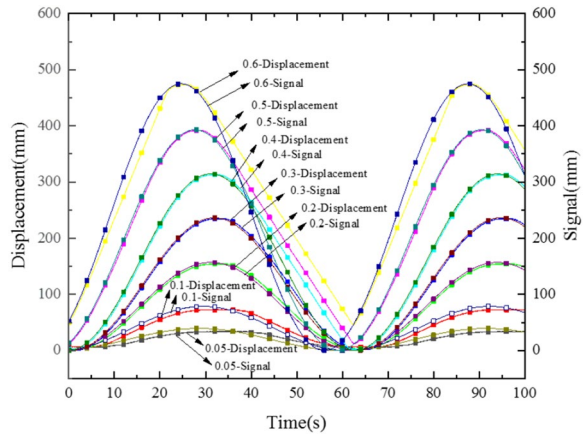

Figure 25 Hydraulic cylinder displacement curve

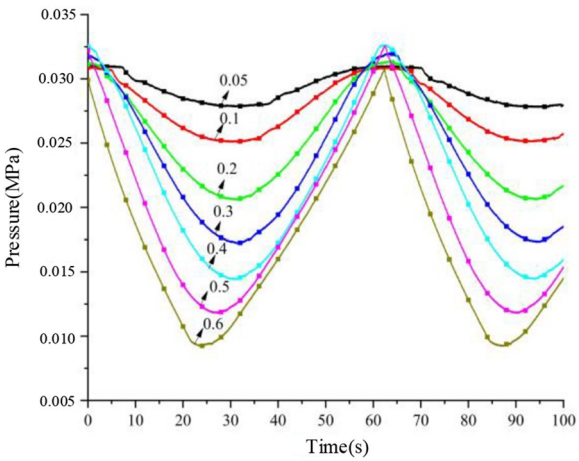

Figure 26 Changes in pressure at different volume ratios

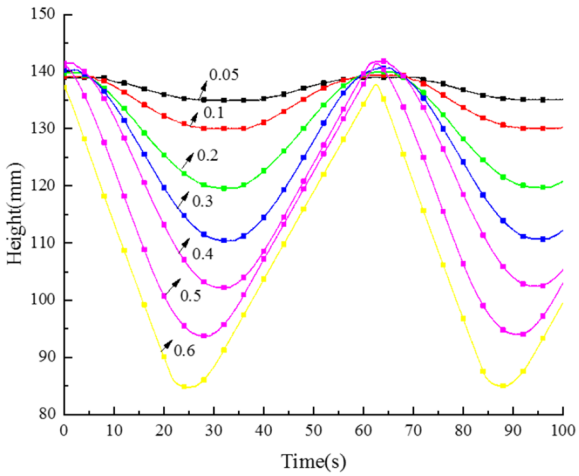

Figure 27 Changes in height at different volume ratios

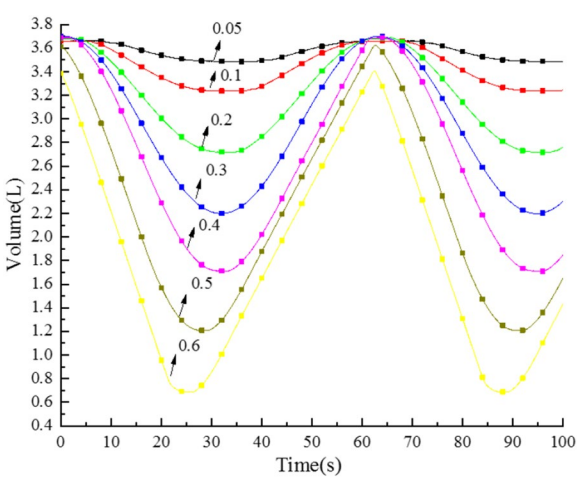

Figure 28 Changes in volume at different volume ratios

of hydraulic systems, such as the natural frequency of the reservoir. Therefore, the improvement of this reservoir will continue on another matching closed-circuit hydraulic system to conduct dynamic tests in the time and frequency domains for further validation and intensive research.

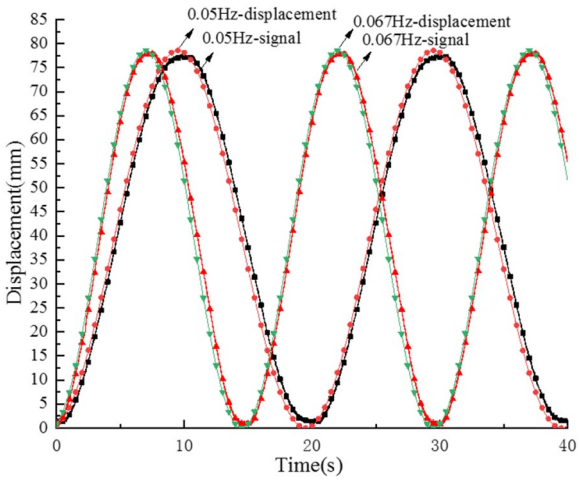

Figure 29 Displacements of the hydraulic cylinder

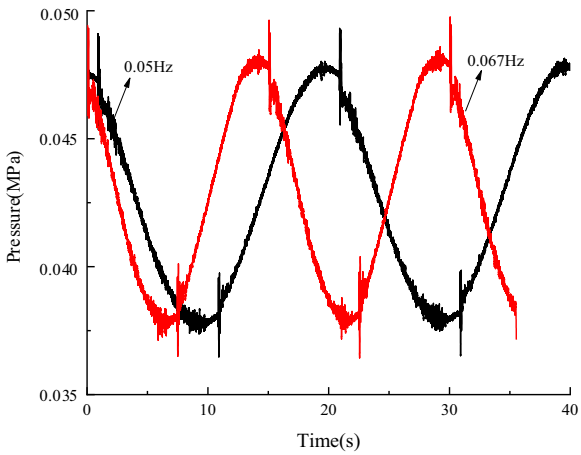

Figure 30 Changes in pressure at different frequencies

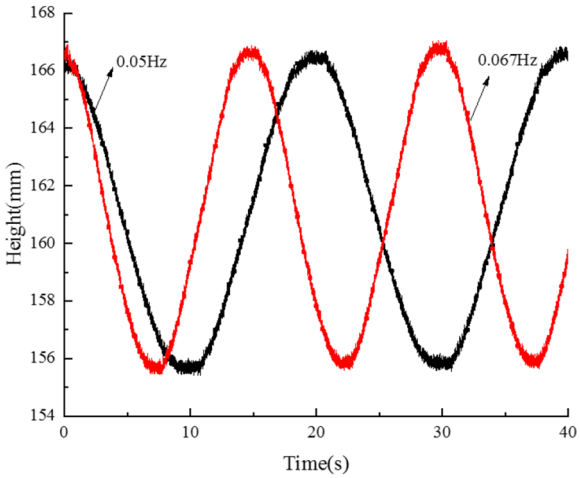

Figure 31 Changes in height at different frequencies

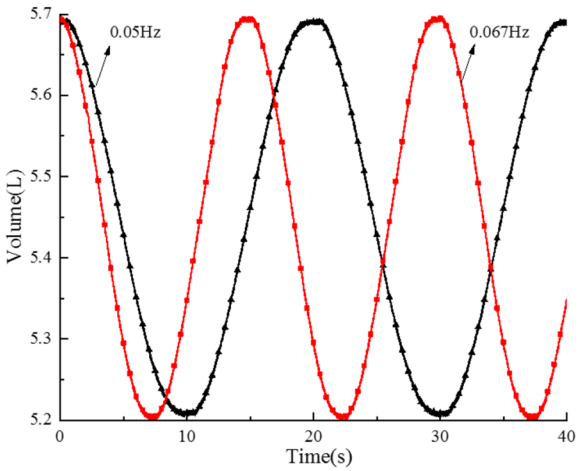

Figure 32 Changes in volume at different frequencies

Acknowledgements
The authors sincerely thank Professor Xiangdong Kong of Yanshan University for his critical discussions and reading during manuscript preparation.

Authors' Information
Pei Wang, born in 1991, is currently a Ph.D. candidate at the *College of Mechanical Engineering, Yanshan University, China*. She received her M.S. degree in 2018 from *Yanshan University, China*. Her research interests include hydraulic system design, fluid transmission, and fluid control.
Jing Yao, born in 1978, is currently a professor at the *College of Mechanical Engineering, Yanshan University, China*. She received her Ph.D. degree in 2009 from *Yanshan University, China*. Her main research interests include hydraulic system control and lightweight hydraulic component design.
Baidong Feng, born in 1994, is currently a master degree candidate at the *College of Mechanical Engineering, Yanshan University, China*. He received his bachelor's degree in 2018 from *Binzhou University, China*. His research interests include hydraulic transmission and hydraulic control.
Mandi Li, born in 1993, is currently a PhD candidate at the *College of Mechanical Engineering, Yanshan University, China*. She received her M.S. degree in 2018 from the *Northeastern University*, China. Her research interests include hydraulic engineering, fluid transmission, fluid simulations, and experiments.
Dingyu Wang, born in 1998, is currently a PhD candidate at the *College of Mechanical Engineering, Yanshan University, China*. He received his bachelor's degree in 2020 from *Yanshan University, China*. His research interests include hydraulic system and machine design.

Author Contributions
JY and PW were in charge of the whole trial; PW and ML wrote the manuscript; and BF and DW assisted with sampling and laboratory analyses. All authors have read and approved the final manuscript.

Funding
Supported by the National Key Research and Development Program of China (Grant No. 2018YFB2000700) and National Natural Science Foundation of China (Grant No. 51890811).

Competing Interests
The authors declare no competing financial interests.

Author Details
[1]School of Mechanical Engineering, Yanshan University, Qinhuangdao 066004, China. [2]Advanced Manufacturing Forming Technology and Equipment, Qinhuangdao 066004, China. [3]Hebei Provincial Key Laboratory of Heavy Fluid Power Transmission and Control, Yanshan University, Qinhuangdao 066004, China.

Received: 7 March 2021 Revised: 15 February 2022 Accepted: 25 March 2022
Published: 11 April 2022

References
[1] Q J Gao. Adaptive control system of underground hydraulic supports. *Energy and Energy Conservation*, 2020(10): 135-136.
[2] Y X Guo, L Zhang. Hybrid power drive system of large die forging hydraulic press. *Forging & Stamping Technology*, 2020, 45(10): 124-129.
[3] Y E Wang, Y Liu, Y Ma, et al. Application of hydraulic steering system for heavy-duty mobile robot. *Hydraulics Pneumatics & Seals*, 2020, 40(9): 24-25.
[4] Q F He, X H Chen, C J Yao, et al. Fault diagnosis expert system of construction machinery based on flowchart knowledge representation. *Machine Tool & Hydraulics*, 2019, 47(17): 216-219.
[5] D J Yang, X B Jin, Z C Yang, et al. Optimization of sensor layout in aero-hydraulic system based on MINIP model. *Measurement & Control Technology*, 2020, 39(5): 49-53.
[6] X D Kong, Q X Zhu, J Yao, et al. Reviews of lightweight development of hydraulic components and systems for high-level mobile equipment. *Journal of Yanshan University*, 2020, 44(3): 203–217.
[7] L F Jiao, X H Lu. Improvement and reliability modeling analysis of aviation hydraulic oil tank sealing structure. *Lubrication Engineering*, 2015, 40(7): 115-120.
[8] L Li, W S Sun, P Gao. Analysis and prevention of common faults about aircraft hydraulic oil Tank. *New Technology & New Process*, 2014(2): 122-124.
[9] R J Liu, F Xu, X Cheng. Test selection and analysis of the hydraulic tank sealing ring of a Helicopter. *Helicopter Technique*, 2019(2): 33-36.
[10] T Li, H L Yang, D B Han. Design and analysis of reservoir for civil aircraft hydraulic system. *Chinese Hydraulics & Pneumatics*, 2017(2): 101-106.
[11] Y Zhang, Y M Wen, S. Wang. Research and experiment of multifunction aero hydraulic tank. *Chinese Hydraulics & Pneumatics*, 2018(11): 104-107.
[12] X P OuYang, B Q Fan, H Y Yang, et al. A novel multi-objective optimization method for the pressurized reservoir in hydraulic robotics. *Journal of Zhejiang University-Science A(Applied Physics & Engineering)*, 2016, 17(6): 454-467.
[13] D X Zhao, T Jia, Y X Cui. Design and constant pressure characteristics of a ship-borne pressure tank. *Tsinghua Univ (Sci & Technol)*, 2019, 59(4): 306-313.
[14] G F Qi, J J Zhang, J G Sun. Miniaturization trend of the hydraulic fuel tank and the new trend of development. *Machine Tool & Hydraulics*, 2011, 39(24): 66–68, 104.
[15] W J Xiao, H Hu, L J Wei. Hydraulic tank of a fighter: fault analysis and improvement. *Chinese Hydraulics & Pneumatics*, 2013(10): 58-61.(in Chinese)
[16] T Zhang, X L Xiao. Troubleshooting of pipeline blockage for the aircraft tank booster system. *Hydraulics Pneumatics & Seals*, 2019, 39(6): 68-70.
[17] D W Li, Z Z Zuo, Z Liu. Design improvement for hydraulic reservoir pressurization system of a certain type of aircraft. *Chinese Hydraulics & Pneumatics*, 2017(11): 105-108.
[18] W B Qu, C W Han, B Z Feng, et al. Design and application of a closed tank in a pitch hydraulic system. *Chinese Hydraulics & Pneumatics*, 2016, (5): 74-77.
[19] B Guo, G L Zhang, J G Zhang. The development of the underground scraper closed tank. *Chinese Hydraulics & Pneumatics*, 2014(1): 83-84.
[20] W Y Kang. A kind of pressure hydraulic tank. CN201320558868.4 [P]. 2013-09-09.
[21] Z J Feng, J Chen, S C Jiang, et al. Bladder hydraulic tank: CN1804408 [P]. 2006-07-19.
[22] Q G Han, Y B Zhang, S Z Yang. Analysis of closed oil tank of interlocking control hydraulic system. *Metallurgical Equipment*, 2016(4): 78-80.
[23] T J Li, L Y He, Z Wang, et al. Flexible variable volume vacuum tank: CN207225926U [P]. 2018-04-13.
[24] Argo-Hytos. Tank Solutions [EB/OL]. https://www.argo-hytos.com/cn/products/tank-solutions.html, 2020.
[25] Fuel Safe. Auxiliary fuel cell bladder tanks for use in airplanes, UAV, Helicopters [EB/OL]. https://fuelsafe.com/aircraft-fuel-bladders, 2020-10-01.
[26] Tertle-Pac. Collapsible aircraft ferry tanks [EB/OL] https://www.turtlepac.com/products/collapsible-aircraft-ferry-tanks, 2020-10-01.

[27] C Seguin. Variable volume reservoir: US6981523, 2006.
[28] B Kim, S B Lee, J Lee. A comparison among Neo-Hookean model, Mooney-Rivlin model, and Ogden model for chloroprene rubber. *International Journal of Precision Engineering and Manufacturing*, 2012(13): 759-764.
[29] C Bi, Z M Chen, L B Zhang, et al. Mathematical Model and Simulation Analysis of Hydraulic Bladder Accumulator. *Aerospace Manufaturing Technology*, 2017(2):11-15.
[30] M Dong, X T Luan, J L Liang, et al. Dynamis Characteristics Analysis of Absorbing Pulsation for Bladder Accumulator. *Chinese Hydraulics & Pneumatics*, 2019(5):109-116.